J|A|C|S ARTICLES

Published on Web 01/15/2009

Electronic Structure of the Ground and Excited States of the Cu_A Site by NMR Spectroscopy

Luciano A. Abriata,[†] Gabriela N. Ledesma,[†] Roberta Pierattelli,[‡] and Alejandro J. Vila*,[†]

IBR (Instituto de Biología Molecular y Celular de Rosario), Consejo Nacional de Investigaciones Científicas y Técnicas (CONICET), Facultad de Ciencias Bioquímicas y Farmacéuticas, Universidad Nacional de Rosario, Suipacha 531, (S2002LRK) Rosario, Argentina, and Magnetic Resonance Center (CERM) and Department of Chemistry, University of Florence, Via Luigi Sacconi 6, 50019 Sesto Fiorentino (Florence), Italy

Received October 8, 2008; E-mail: vila@ibr.gov.ar

Abstract: The electronic properties of *Thermus thermophilus* Cu_A in the oxidized form were studied by ^1H and ^{13}C NMR spectroscopy. All of the ^1H and ^{13}C resonances from cysteine and imidazole ligands were observed and assigned in a sequence-specific fashion. The detection of net electron spin density on a peptide moiety is attributed to the presence of a H-bond to a coordinating sulfur atom. This hydrogen bond is conserved in all natural Cu_A variants and plays an important role for maintaining the electronic structure of the metal site, rendering the two Cys ligands nonequivalent. The anomalous temperature dependence of the chemical shifts is explained by the presence of a low-lying excited state located about 600 cm^{-1} above the ground state. The room-temperature shifts can be described as the thermal average of a σ_u^* ground state and a π_u excited state. These results provide a detailed description of the electronic structure of the Cu_A site at atomic resolution in solution at physiologically relevant temperature.

Introduction

Cytochrome *c* oxidase (C*c*O) is a membrane-embedded enzymatic complex that catalyzes the reduction of molecular oxygen to water, accepting electrons from reduced cytochrome *c* molecules and contributing to the generation of a transmembrane proton gradient that is used as energy currency for a variety of cellular mechanisms.[1,2] C*c*O is an integral membrane protein located in the inner mitochondrial membrane of eukaryotic cells and in the membrane of prokaryotic cells. It is composed of several subunits, which accommodate a series of cofactors involved in electron transfer from cytochrome *c* to the catalytic center, and in the chemical reaction itself. The catalytic efficiency of C*c*O depends on an efficient electron transport from cytochrome *c* to the reactive heme a_3-Cu_B, buried deep inside the membrane.[1,2] Electrons coming from cytochrome *c* are transferred to a heme group embedded in the membrane by a binuclear copper site (Cu_A),[3−5] which is located on the periplasmic (or intermembrane) side of the C*c*O.

Cu_A is a binuclear metal center with two cysteine ligands bridging the copper ions, two terminal histidine residues coordinated through their Nδ atoms, and two weakly coordinated axial ligands provided by a methionine sulfur and a backbone carbonyl (Figure 1A).[6] The Cys sulfur atoms together with the copper ions give rise to a highly covalent and rigid Cu_2S_2 core, where the copper ions are only 2.4−2.6 Å apart.[7−10] The high efficiency of the Cu_A center in shuttling electrons over long distances has been attributed to the high rigidity of this core, which endows it with a low reorganization energy,[11,12] and to

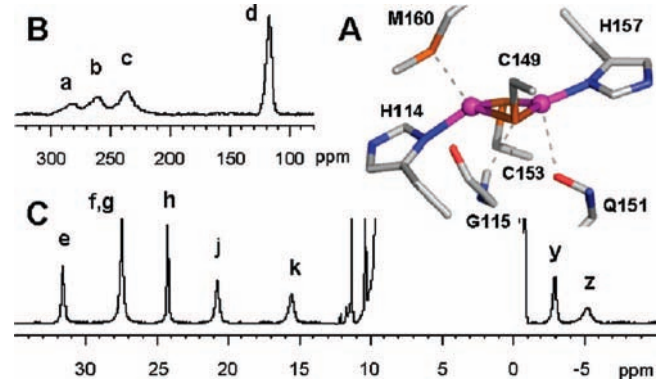

Figure 1. (A) The binuclear CuA center rendered from PDB ID 2CUA.[7] (B and C) ^1H NMR spectra of unlabeled *Tt*Cu_A, aimed to detect the paramagnetically shifted signals a−d (B, recorded with SuperWEFT sequence) and e−z (C, recorded with presaturation of the water signal). Spectra recorded at 600 MHz, 298 K, on a sample at pH 7 in water.

[†] Universidad Nacional de Rosario.
[‡] University of Florence.

(1) Ferguson-Miller, S.; Babcock, G. T. *Chem. Rev.* **1996**, *96*, 2889–2907.
(2) Wikstrom, M. *Biochim. Biophys. Acta* **2004**, *1655*, 241–247.
(3) Muresanu, L.; Pristovsek, P.; Lohr, F.; Maneg, O.; Mukrasch, M. D.; Ruterjans, H.; Ludwig, B.; Lucke, C. *J. Biol. Chem.* **2006**, *281*, 14503–14513.
(4) Maneg, O.; Ludwig, B.; Malatesta, F. *J. Biol. Chem.* **2003**, *278*, 46734–46740.
(5) Abriata, L. A.; Banci, L.; Bertini, I.; Ciofi-Baffoni, S.; Gkazonis, P.; Spyroulias, G. A.; Vila, A. J.; Wang, S. *Nat. Chem. Biol.* **2008**, *4*, 599–601.
(6) Beinert, H. *Eur. J. Biochem.* **1997**, *245*, 521–532.
(7) Williams, P. A.; Blackburn, N. J.; Sanders, D.; Bellamy, H.; Stura, E. A.; Fee, J. A.; McRee, D. E. *Nat. Struct. Biol.* **1999**, *6*, 509–516.
(8) Soulimane, T.; Buse, G.; Bourenkov, G. P.; Bartunik, H. D.; Huber, R.; Than, M. E. *EMBO J.* **2000**, *19*, 1766–1776.

its particular electronic structure.[13,14] The reduced [$Cu^{1+}-Cu^{1+}$] state is diamagnetic, while the oxidized form [$Cu^{1.5+}-Cu^{1.5+}$] is a fully delocalized class III mixed-valence pair with two equivalent copper ions as put forward by Kroneck, Antholine, and co-workers by EPR before the availability of a crystal structure.[15,16] The strong Cu−S bonding has been supported by the large covalence evidenced by XAS studies at the Cu and S edges from the Solomon group,[17−22] as well as by ENDOR[23−25] and NMR data,[26−31] which have revealed a large amount of unpaired spin density onto the Cys residues.

All spectroscopic evidence and theoretical calculations support a σ_u* ground state and a π_u level as the first excited state.[17,19,32−36] This description is consistent with the short Cu−Cu distance (2.4−2.6 Å), which also allows full valence delocalization in the oxidized state despite the asymmetry of the protein milieu. Instead, a dinuclear copper model complex synthesized by Tolman with a longer Cu−Cu distance (2.92 Å) displays an inversion of these two levels, with the π_u becoming the ground state.[19] The value of the σ_u^*/π_u energy gap in Cu_A centers has been a matter of debate:[33] EPR and MCD spectra are consistent with a value of 5000 cm^{-1}, while the unusual temperature dependence of the NMR spectra was interpreted as the result of the existence of a thermally accessible excited state located at 200−800 cm^{-1}.[27,30,31]

In recent years, an emerging concept in biochemistry has arisen from NMR studies: the identification and characterization of excited states that become populated at room temperature.[37,38] The availability of these states allows the protein to explore alternative conformations relevant for protein folding, substrate recognition, and catalysis. In paramagnetic metalloproteins, the interrogation of the electronic structures of excited states by room-temperature spectroscopic techniques has been valuable to account for the existence of low lying excited states in heme systems,[39,40] iron−sulfur clusters,[41] and dinuclear Cu(II) centers.[42−44] Notwithstanding, the issue of the excited state in native Cu_A sites has been rather elusive and debated. Here, we report an extensive, unambiguous assignment of the ^1H and ^{13}C NMR spectra of the Cu_A fragment from *Thermus thermophilus* ba_3 oxidase (*Tt*Cu_A). These data allow us to (1) calculate the energy gap between the ground and excited states at room temperature and explain the anomalous temperature dependence of the ^{13}C signals; (2) identify these states as those predicted from quantum mechanical calculations; (3) estimate the experimental electron spin density of the thermally averaged species resulting at room temperature; (4) provide a description of the electron spin density at the σ_u* and π_u states; and (5) detect electron spin density delocalized by H-bonding to a sulfur atom of one Cys, which plays an important role in maintaining the electronic structure of the center and makes the two Cys ligands nonequivalent. These findings provide new insights for the understanding of the electronic structure of the Cu_A site and its possible role in long-range electron transfer events, as well as for the complementary nature of ground-state magnetic techniques (such as EPR, ENDOR, and MCD) with solution NMR, a room-temperature technique.

Materials and Methods

Production of Protein Samples. Unlabeled and uniformly labeled proteins were expressed from pET9ACuAWTT9 (Kan^R) in *E. coli* BL21(DE3) growing in either rich LB medium or M9 minimal medium supplemented with labeled or unlabeled ammonium sulfate (1.2 g/L, 99% ^{15}N when labeled) and glucose (4

(9) Tsukihara, T.; Aoyama, H.; Yamashita, E.; Tomizaki, T.; Yamaguchi, H.; Shinzawa-Itoh, K.; Nakashima, R.; Yaono, R.; Yoshikawa, S. *Science* **1996**, *272*, 1136–1144.
(10) Iwata, S.; Ostermeier, C.; Ludwig, B.; Michel, H. *Nature* **1995**, *376*, 660–669.
(11) Farver, O.; Hwang, H. J.; Lu, Y.; Pecht, I. *J. Phys. Chem. B* **2007**, *111*, 6690–6694.
(12) Farver, O.; Lu, Y.; Ang, M. C.; Pecht, I. *Proc. Natl. Acad. Sci. U.S.A.* **1999**, *96*, 899–902.
(13) Solomon, E. I.; Xie, X.; Dey, A. *Chem. Soc. Rev.* **2008**, *37*, 623–638.
(14) Randall, D. W.; Gamelin, D. R.; LaCroix, L. B.; Solomon, E. I. *J. Biol. Inorg. Chem.* **2000**, *5*, 16–29.
(15) Kroneck, P. M.; Antholine, W. E.; Kastrau, D. H.; Buse, G.; Steffens, G. C.; Zumft, W. G. *FEBS Lett.* **1990**, *268*, 274–276.
(16) Kroneck, P. M. H.; Antholine, W. E.; Riester, J.; Zumft, W. G. *FEBS Lett.* **1988**, *242*, 70–74.
(17) de Beer, S.; Markus, M.; Wang, H.; Wang, H.; Cramer, S. P.; Lu, Y.; Tolman, W. B.; Hedman, B.; Hodgson, K. O.; Solomon, E. I. *J. Am. Chem. Soc.* **2001**, *123*, 5757–5767.
(18) Antholine, W. E.; Kastrau, D. H. W.; Steffens, G. C. M.; Buse, G.; Zumft, W. G.; Kroneck, P. M. H. *Eur. J. Biochem.* **1992**, *209*, 875–881.
(19) Gamelin, D. R.; Randall, D. W.; Hay, M. T.; Houser, R. P.; Mulder, T. C.; Canters, G. W.; De Vries, S.; Tolman, W. B.; Solomon, E. I. *J. Am. Chem. Soc.* **1998**, *120*, 5246–5263.
(20) Williams, K. R.; Gamelin, D. R.; LaCroix, L. B.; Houser, R. P.; Tolman, W. B.; Mulder, T. C.; De Vries, S.; Hedman, B.; Hodgson, K. O.; Solomon, E. I. *J. Am. Chem. Soc.* **1997**, *119*, 613–614.
(21) Blackburn, N. J.; De Vries, S.; Barr, M. E.; Houser, R. P.; Tolman, W. B.; Sanders, D.; Fee, J. A. *J. Am. Chem. Soc.* **1997**, *119*, 6135–6143.
(22) Blackburn, N. J.; Barr, M. E.; Woodruff, W. H.; van der Oost, J.; De Vries, S. *Biochemistry* **1994**, *33*, 10401–10407.
(23) Gurbiel, R. J.; Fann, Y. C.; Surerus, K. K.; Werst, M. M.; Musser, S. M.; Doan, P. E.; Chan, S. I.; Fee, J. A.; Hoffman, B. M. *J. Am. Chem. Soc.* **1993**, *115*, 10888–10894.
(24) Epel, B.; Slutter, C. S.; Neese, F.; Kroneck, P. M.; Zumft, W. G.; Pecht, I.; Farver, O.; Lu, Y.; Goldfarb, D. *J. Am. Chem. Soc.* **2002**, *124*, 8152–8162.
(25) Slutter, C. E.; Gromov, I.; Epel, B.; Pecht, I.; Richards, J. H.; Goldfarb, D. *J. Am. Chem. Soc.* **2001**, *123*, 5325–5332.
(26) Holz, R. C.; Alvarez, M. L.; Zumft, W. G.; Dooley, D. M. *Biochemistry* **1999**, *38*, 11164–11171.
(27) Salgado, J.; Warmerdam, G. C.; Bubacco, L.; Canters, G. W. *Biochemistry* **1998**, *37*, 7378–7389.
(28) Dennison, C.; Berg, A.; Canters, G. W. *Biochemistry* **1997**, *36*, 3262–3269.
(29) Luchinat, C.; Soriano, A.; Djinovic, K.; Saraste, M.; Malmström, B. G.; Bertini, I. *J. Am. Chem. Soc.* **1997**, *119*, 11023–11027.
(30) Bertini, I.; Bren, K. L.; Clemente, A.; Fee, J. A.; Gray, H. B.; Luchinat, C.; Malmström, B. G.; Richards, J. H.; Sanders, D.; Slutter, C. E. *J. Am. Chem. Soc.* **1996**, *118*, 11658–11659.
(31) Fernandez, C. O.; Cricco, J. A.; Slutter, C. E.; Richards, J. H.; Gray, H. B.; Vila, A. J. *J. Am. Chem. Soc.* **2001**, *123*, 11678–11685.
(32) Xie, X.; Gorelsky, S. I.; Sarangi, R.; Garner, D. K.; Hwang, H. J.; Hodgson, K. O.; Hedman, B.; Lu, Y.; Solomon, E. I. *J. Am. Chem. Soc.* **2008**, *130*, 5194–5205.
(33) Gorelsky, S. I.; Xie, X.; Chen, Y.; Fee, J. A.; Solomon, E. I. *J. Am. Chem. Soc.* **2006**, *128*, 16452–16453.
(34) Farrar, J. A.; Neese, F.; Lappalainen, P.; Kroneck, P. M. H.; Saraste, M.; Zumft, W. G.; Thompson, A. J. *J. Am. Chem. Soc.* **1996**, *118*, 11501–11514.
(35) Neese, F.; Zumft, W. G.; Antholine, W. A.; Kroneck, P. M. H. *J. Am. Chem. Soc.* **1996**, *118*, 8692–8699.
(36) Olsson, M. H.; Ryde, U. *J. Am. Chem. Soc.* **2001**, *123*, 7866–7876.
(37) Korzhnev, D. M.; Kay, L. E. *Acc. Chem. Res.* **2008**, *41*, 442–451.
(38) Boehr, D. D.; McElheny, D.; Dyson, H. J.; Wright, P. E. *Science* **2006**, *313*, 1638–1642.
(39) Banci, L.; Bertini, I.; Luchinat, C.; Pierattelli, R.; Shokhirev, N. V.; Walker, F. A. *J. Am. Chem. Soc.* **1998**, *120*, 8472–8279.
(40) Shokhirev, N. V.; Walker, F. A. *J. Phys. Chem.* **1995**, *99*, 17795–17804.
(41) Banci, L.; Bertini, I.; Luchinat, C. *Struct. Bonding (Berlin)* **1990**, *72*, 113–135.
(42) Tepper, A. W.; Bubacco, L.; Canters, G. W. *Chemistry* **2006**, *12*, 7668–7675.
(43) Bubacco, L.; Salgado, J.; Tepper, A. W.; Vijgenboom, E.; Canters, G. W. *FEBS Lett.* **1999**, *442*, 215–220.
(44) Murthy, N. N.; Karlin, K. D.; Bertini, I.; Luchinat, C. *J. Am. Chem. Soc.* **1997**, *119*, 2156–2162.

g/L, 99% ^{13}C when labeled), respectively, according to the desired labeling scheme. Proteins with ^{13}C and ^{15}N labeling at Cys were expressed from the same plasmid in *E. coli* JM15(DE3)pLysS (*Cm*^{R}) in M9 minimal medium supplemented with unlabeled ammonium sulfate (1.2 g/L) and glucose (4 g/L), doubly labeled cysteine ($^{15}NH_2{}^{13}CH(^{13}CH_2SH)^{13}COOH$), and the 19 remaining unlabeled amino acids as detailed in refs 45, 46. Typical yields were about 13 and 30 mg/L for labeled and unlabeled samples, respectively.

Purification of proteins from cell lysates was done as described elsewhere.[31,47] Protein samples for NMR experiments were prepared in 100 mM phosphate buffer (pH 7 unless otherwise noted) with 100 mM KCl in either 10% or 100% D_2O as required for each experiment, and concentrated to 250−300 μL of 1−2.5 mM protein concentration.

Nuclear Magnetic Resonance Spectroscopy. NMR experiments were carried out on a Bruker Avance II spectrometer operating at 600.13 MHz (^1H frequency). ^1H-detected spectra were acquired with a triple-resonance (TXI) probehead. ^1H spectra in the 35/−10 ppm region were observed with a $\pi/2$ pulse preceded by presaturation of the water signal, on a spectral window of ca. 48 kHz, and with a total recycle time of ca. 300 ms. ^1H spectra aimed at the observation of the broad Hβ Cys signals were acquired with a SuperWEFT pulse sequence[48] on a spectral window of ca. 360 kHz, with a total recycle delay of ca. 40 ms and different intermediate delays. $^1H,^{13}C$- and $^1H,^{15}N$-HMQC experiments were acquired on spectral widths of ca. 50 kHz in the ^1H dimension (1k points) and ca. 100 kHz in the indirect dimension (128 points). The delay for coherence transfer was set to the average T_2 of the involved ^1H signals, that is, about 2 ms, and the relaxation delay was set to ca. 30 ms.[49] Several experiments were carried out setting the frequency of the heteronucleus at different offsets.

Saturation transfer difference and NOE experiments on the broad signals from Cys' β protons were performed on samples prepared in 100% D_2O buffer, either completely oxidized for NOE experiments or partially reduced for saturation transfer difference experiments (ca. 10% reduced protein, obtained by addition of a suitable substoichometric amount of sodium ascorbate). All of these spectra were acquired using the reported experimental scheme,[50] irradiating the signal of interest for ca. 50 ms at a power of ca. 5 mW. The total recycle time was ca. 75 ms.

Carbon-13 detected spectra were acquired with a broadband observe (BBO) probehead tuned at the proper frequency, using an excitation pulse of 6.9 μs at 88.67 W. Inverse gated decoupling was applied during acquisition of ^{13}C spectra. For ^{13}C experiments, the carrier frequency was set to 800, 300, or −500 ppm depending on which signals were being studied at the moment. The spectral window and delays also varied in each experiment, resulting in total recycle times of ca. 35 ms for the acquisition of signals around 800 and −500 ppm, and ca. 300 ms for those near the diamagnetic region. No further signals were detected when the carrier was moved to different frequency offsets.

Saturation transfer difference experiments on ^{13}C signals were performed on samples containing ca. 10% reduced protein (obtained by addition of a suitable substoichiometric amount of sodium ascorbate). Saturation transfer difference spectra were acquired with the same pulse sequence used for protons but adapted to the ^{13}C channel, irradiating during ca. 40 ms at a power of ca. 0.1−5 mW. Total recycle time was ca. 70 ms.

Calculation of Electron−Nuclei Coupling Constants. The electron−nuclei coupling constant (A/h) for each nucleus can be calculated from the contact shift using the following equation:[51,52]

$$\frac{A}{h} = \frac{3\gamma k_B \delta_{contact} T}{2\pi \bar{g} \mu_B S(S+1)} \quad (1)$$

where γ is the nuclear gyromagnetic ratio, k_B is Boltzmann's constant, $\bar{g}$ is the average of the **g** tensor components, μ_B is the Bohr magneton, S is the electronic spin ($^1/_2$ for the oxidized Cu_A center), and T is the temperature in Kelvin. It should be noted that eq 1 is valid for an isolated spin state.[53] This is not the case here, and we will use the obtained apparent electron−nuclei coupling constant ($(A/h)_{app}$) for comparison purposes with similar systems. $\delta_{contact}$ is the contact contribution to the chemical shift, which is calculated, in turn, from the observed chemical shift as:

$$\delta_{contact} = \delta_{obs} - \delta_{diamagnetic} - \delta_{pseudocontact} \quad (2)$$

In the case of *Tt*Cu_A, the full assignment of the reduced protein to retrieve the diamagnetic shifts is available (BMRB entry 5819),[54] while the pseudocontact shifts can be estimated from EPR data using eq 3:

$$\delta_{pseudocontact} = \frac{\mu_0}{4\pi}\frac{\mu_B^2 S(S+1)}{9k_B T r^3}(3\cos^2\theta - 1)(g_{\parallel}^2 - g_{\perp}^2) \quad (3)$$

where μ_0 is the vacuum permeability, r is the module of a vector **r** connecting the nucleus and the averaged coordinates of both copper ions, θ is the angle between the z component of the **g** tensor and the **r** vector, and $g_{\parallel}$ and $g_{\perp}$ are the parallel and perpendicular values of the axial **g** tensor. Strictly speaking, it would be appropiate to use the principal components of the molecular susceptibility tensor χ instead of the components of the **g** tensor; however, this approximation is acceptable for null or small spin−orbit coupling. The magnetic axes were defined as described by Neese and coworkers.[35] The other terms were defined in eq 1. The pseudocontact shift proved to be small in all cases (cf., Table 2), as expected.

Fitting of Temperature Dependence Data. The temperature dependence data were fitted to a two-states model using the program TDFw,[40] which calculates the contact contribution to the chemical shift for each data point and fits all data at once to the following equation:

$$\delta_{contact,k} = \frac{1}{T}\frac{f_{k,1} + f_{k,2}e^{(-\Delta E/k_B T)}}{1 + e^{(-\Delta E/k_B T)}} \quad (4)$$

Fitting the data to this equation yields $f_{k,i}$, contribution of nucleus k to the contact shift in the state i ($i = 1$ for ground state, $i = 2$ for excited state), and ΔE, the energy gap between the two states.

Results

^1H NMR Spectra of *Tt*Cu_A Samples Produced under Various Labeling Schemes. The ^1H NMR spectrum of *Tt*Cu_A (Figure 1) displays a number of isotropically shifted signals, which can be clustered into two groups on the basis of the extent of the paramagnetic effect they are subject to. The first group includes a set of relatively sharp signals with chemical shifts ranging from 32 to 15 ppm (e−k) and from −3 to −7 ppm (y, z). The second group includes four broad signals with chemical shifts between ca. 300 and 110 ppm (a−d). This spectrum,

(45) Cheng, H.; Westler, W. M.; Xia, B.; Oh, B.-H.; Markley, J. L. *Arch. Biochem. Biophys.* **1995**, *316*, 619–634.
(46) Bertini, I.; Jonsson, B.-H.; Luchinat, C.; Pierattelli, R.; Vila, A. J. *J. Magn. Reson., Ser. B* **1994**, *104*, 230–239.
(47) Slutter, C. E.; Sanders, D.; Wittung, P.; Malmström, B. G.; Aasa, R.; Richards, J. H.; Gray, H. B.; Fee, J. A. *Biochemistry* **1996**, *35*, 3387–3395.
(48) Inubushi, T.; Becker, E. D. *J. Magn. Reson.* **1983**, *51*, 128–133.
(49) Banci, L.; Bertini, I.; Pierattelli, R.; Vila, A. J. *Inorg. Chem.* **1994**, *33*, 4338–4343.
(50) Banci, L.; Bertini, I.; Luchinat, C.; Piccioli, M.; Scozzafava, A.; Turano, P. *Inorg. Chem.* **1989**, *28*, 4650–4656.
(51) Bertini, I.; Luchinat, C. *NMR of Paramagnetic Substances*; Elsevier: Amsterdam, 1996.
(52) McConnell, H. M.; Chesnut, D. B. *J. Chem. Phys.* **1958**, *28*, 107–117.
(53) Kurland, R. J.; McGarvey, B. R. *J. Magn. Reson.* **1970**, *2*, 286–301.
(54) Mukrasch, M. D.; Lucke, C.; Lohr, F.; Maneg, O.; Ludwig, B.; Ruterjans, H. *J. Biomol. NMR* **2004**, *28*, 297–298.

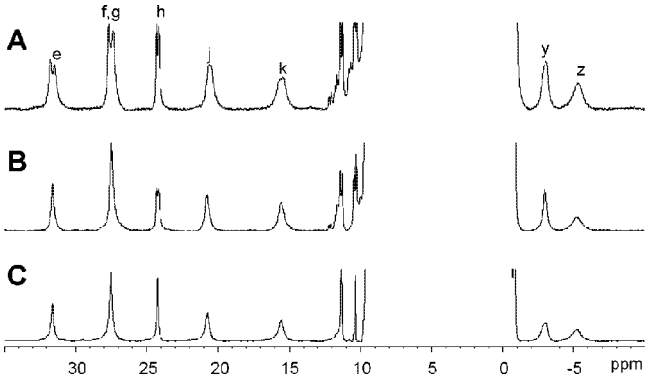

Figure 2. ^{1}H NMR spectra of *Tt*Cu$_A$ uniformly labeled with ^{13}C and ^{15}N (A), uniformly labeled with ^{15}N (B), and doubly labeled at Cys (C), registered at 298 K.

already reported and partially assigned by Bertini and coworkers,[30] exhibits the same pattern of ^{1}H signals observed for all studied Cu$_A$-containing proteins.[26−31]

On the basis of their NOE patterns and their distinct solvent exchange properties, signals e, f, h, j, and k had been unambiguously assigned to specific protons from the imidazole rings of His114 and His157.[30] Resonances a−d had been assigned to the β-CH$_2$ moieties of the Cys ligands, based on their large chemical shifts and line widths[30] (and later confirmed by selective deuteration of the Cys ligands).[29] Resonance g had been attributed to one of the two α-CH Cys based on the unusual temperature dependence of its chemical shift. The sequence-specific assignment of all of the identified cysteines' signals, as well as the identification of the second α-CH Cys, had not been obtained at that time based on the ^{1}H NMR data available. The upfield resonances y and z (the latter slowly exchangeable with solvent) remained unassigned as well.

Figure 2 shows the 35 to −10 ppm region of the ^{1}H NMR spectra of *Tt*Cu$_A$ samples obtained by using different labeling schemes. As these resonances are relatively sharp, heteronuclear ^{1}H,^{13}C and ^{1}H,^{15}N splittings could be measured. The splittings observed for resonances e, f, h, j, and k in the ^{13}C,^{15}N and ^{15}N labeled samples (Figure 2A and B, respectively) provide further confirmation of their assignment. The broadening experienced by signals g and y in the selectively ^{13}C,^{15}N labeled Cys sample supports the assignment of the former as a Cys Hα (Supporting Information, Figure S1) and reveals that the latter is also due to a carbon-bound Cys proton, most likely the other Cys Hα.

Direct and Inverse Detection Heteronuclear Experiments and Assignment of ^{13}C NMR Signals. A number of paramagnetically shifted ^{13}C signals spanning a chemical shift range of 1400 ppm (from ca. 900 to −500 ppm) were observed in the spectrum recorded with the ^{13}C,^{15}N-uniformly labeled sample (Figure 3A,B,D). To optimize detection of the most downfield (A) and most upfield (Y, Z) shifted resonances, spectra were recorded with frequency offsets located close to the signals of interest, as described in the caption of Figure 3. Instead, resonances in the 400−0 ppm regions could be detected with the frequency offset located at 300 ppm.

Carbon-13 spectra recorded on the ^{13}C,^{15}N selectively labeled Cys sample revealed the presence of the hyperfine-shifted signals A, F, Y, and Z, in addition to a group of eight resonances in the diamagnetic region (Figure 3C), which were not resolved in the spectrum of a fully labeled sample. Six of these signals were already assigned to ^{13}C nuclei from the Cys ligands in the reduced form.[3] Signals I and J remained unassigned at this stage and may be attributed to signals of the oxidized species.

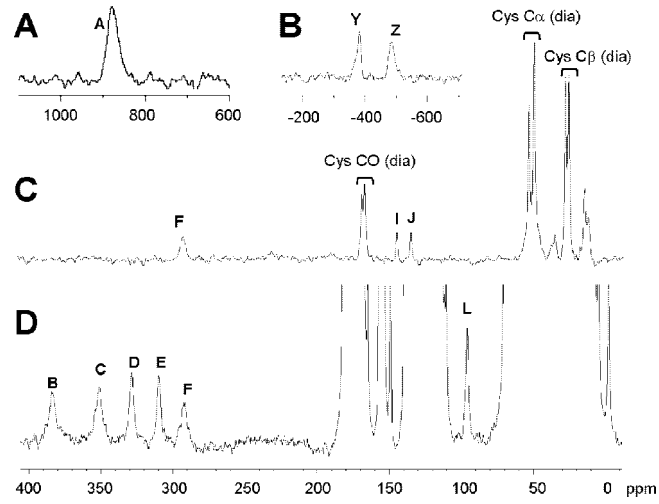

Figure 3. ^{13}C NMR spectra of *Tt*Cu$_A$ labeled at Cys (A, B, C) and of uniformly labeled *Tt*Cu$_A$ (D) recorded at 298 K. The spectrum where signal A is seen (A) was acquired with the offset of the carbon channel set at 800 ppm and processed with 800 Hz line broadening. The spectrum showing signals Y and Z (B) was acquired with the offset at −500 ppm and processed with 1000 Hz of line broadening. Spectra spanning from 400 to −10 ppm (C, D) were acquired with the offset at 300 ppm and processed with 100 Hz line broadening.

A ^{1}H,^{13}C HMQC spectrum performed on the uniformly labeled sample, recorded under conditions tailored to detect the heteronuclear coherences corresponding to paramagnetic signals (Supporting Information, Figure S2), allowed us to assign signal B to the Cδ2 of His157 (correlating with the proton signal f), signal C to the Cδ2 of His114 (correlating with e), and signal F to the Cys149 Cα (correlating with y). This HMQC also allowed us to resolve the ^{13}C signals L and M, which were hidden in the diamagnetic envelope in the 1D ^{13}C NMR spectrum, and to assign them to the His157 Cε1 (L, connected to k) and His114 Cε1 (M, connected to j). These correlations were further verified by recording 1D ^{1}H experiments in which each of the ^{13}C signals was selectively irradiated, and monitoring the collapse of the doublet in the ^{1}H spectrum (Supporting Information, Figure S3).

To complete the assignment of the signals resolved in the ^{13}C spectrum, we recorded a series of 1D saturation transfer difference experiments. Saturation of signal D gives a response in the diamagnetic region at 136.5 ppm, which corresponds to His157Cγ, while saturation of signal E shows transfer to a signal at 135.5 ppm due to His114Cγ. Irradiation of signals A and F resulted in saturation transfer to signals at 56.5 and 59.9 ppm, which correspond to Cys153Cα and Cys149Cα, respectively. Finally, saturation transfer experiments performed on signals Y and Z yielded responses at 32.3 and 34.5 ppm, which arise from Cys149Cβ and Cys153Cβ, respectively. The saturation transfer difference experiments aimed at the assignment of signals I and J were performed on the sample selectively labeled at Cys and demonstrate that these signals correspond to Cys149CO and J to Cys153CO in the oxidized form, respectively (Figure 4).

This combination of direct and inverse ^{13}C experiments allowed us to complete the assignment of the ^{13}C resonances of the two His and the two Cys ligands, including the quaternary carbons from the imidazole rings and those bound to protons giving broad signals such as the Cys' Cβs. The assignment of all ^{13}C resonances is summarized in Table 1, together with the

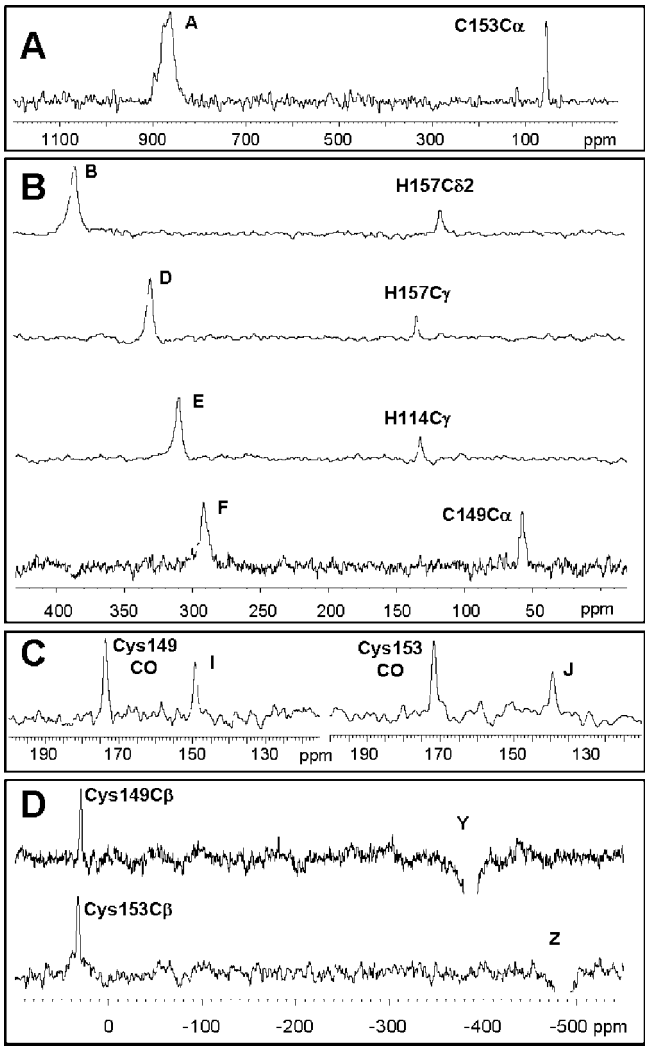

Figure 4. Saturation transfer difference spectra obtained by irradiation of ^{13}C resonances A (panel A), B, D, E, F (panel B), Y and Z (panel D) on a fully labeled sample, and I and J (panel C) on a sample labeled at the cysteine residues. Experiments were performed at 298 K.

relaxation times and the temperature dependence of their chemical shifts.

Sequence-Specific Assignment of ^1H Resonances. The ^{13}C saturation transfer experiments described in the previous section reveal that the most downfield shifted signal, A, corresponds to the Cys153Cα, while signal F is due to the Cys149Cα. A cross peak between signals F and y in the HMQC spectrum (Supporting Information, Figure S2) allows us to unambiguously assign signal y to the Hα of Cys149. On the basis of its unusual temperature dependence, Bertini et al. tentatively assigned signal g to the Hα of a Cys ligand.[30] The absence of any correlation for that signal in the ^1H,^{13}C HMQC spectrum led us to record ^{13}C-filtered ^1H experiments on the sample selectively labeled at the Cys residues with the offset of the ^{13}C channel set close to the shifted resonance (Supporting Information, Figure S4). When the ^{13}C offset was set at 800 ppm (signal A), only signal g was found in the ^1H spectrum. Instead, when the ^{13}C offset was located at 300 ppm (signal F), only signal y was detected. These experiments thus permit one to assign signal y to Cys149Hα and to confirm the assignment of resonance g to Cys153Hα.

Assignment of the broad resonances a−d (in the 290−115 ppm region, Figure 1) arising from the Hβ protons of the cysteines to either Cys153 or Cys149 could be pursued by using a combined strategy. A series of NOE experiments were performed on these resonances on a fully oxidized sample. These experiments show that signals a and d both present a common NOE with signal g (Cys153Hα), suggesting that signals a and d arise from the β protons of Cys153. Instead, signals b and c share an NOE with signal y (Cys149Hα) (Supporting Information, Figure S5), allowing us to assign b and c to the Hβs of Cys149. These assignments were further confirmed by carrying out a series of saturation transfer difference ^1H experiments on resonances a−d in a sample partially reduced with ascorbate (Supporting Information, Figure S6), based on the ^1H assignments on the reduced protein.

Table 1. Assignment of ^1H, ^{13}C, and ^{15}N Resonances of Oxidized *Tt*Cu_A[a]

	signal	δ_{obs} (ppm)	line width (Hz)	temperature dependence	assignment
^{13}C	A	881	3900	hyper-Curie	Cys153Cα
	B	386.2	576	hyper-Curie	His157Cδ2
	C	353.6	772	hyper-Curie	His114Cδ2
	D	331.2	380	Curie	His157Cγ
	E	312.2	340	hypo-Curie	His114Cγ
	F	294.6	728	anti-Curie	Cys149Cα
	I	151.7	103	hyper-Curie	Cys149CO
	J	142.0	63	hyper-Curie	Cys153CO
	L	98.4	223	hypo-Curie	His157Cε1
	M	33.9	ND[c]	ND[c]	His114Cε1
	Y	−379	1800	hypo-Curie	Cys149Cβ
	Z	−475	2500	hypo-Curie	Cys153Cβ
^1H	a	283	7200	hyper-Curie	Cys153Hβ
	b	262	5300	hypo-Curie	Cys149Hβ
	c	237	5900	hyper-Curie	Cys149Hβ
	d	117	3100	anti-Curie	Cys153Hβ
	e	31.6	114	Curie	His114Hδ2
	f	27.46	ND[c]	hyper-Curie	His157Hδ2
	g	27.55	ND[c]	*T*-independent	Cys153Hα
	h	24.2	52	Curie	His114Hε2
	i[b]	23.2	170	Curie	His157Hε2
	j	20.7	165	hyper-Curie	His114Hε1
	k	15.5	210	hyper-Curie	His157Hε1
	y	−2.9	144	hyper-Curie	Cys149Hα
	z	−5.2	374	Curie	Gly115HN

[a] Observed chemical shifts, line widths, and temperature dependence are reported at 298 K. [b] Signal i is observed at low pH and temperatures. [c] ND: not determined.

The ^1H NMR spectra of oxidized Cu_A centers present an upfield-shifted signal around −5 to −10 ppm, broader than any other signal in the 35 to −10 ppm range. This resonance exchanges very slowly in D_2O, suggesting that it corresponds to a proton involved in a strong hydrogen bond. To assign signal z, we performed a saturation transfer difference experiment on a partially reduced sample. This experiment yielded a response at 10.1 ppm (Supporting Information, Figure S7), which corresponds to the backbone HN of Gly115 in the reduced protein. Inspection of the *Tt*Cu_A site (PDB ID 2CUA) shows that this HN is involved in a hydrogen bond with the S atom of Cys149, suggesting the presence of unpaired spin density transmitted through hydrogen bonds (Figure 1A).

Temperature Dependence of the Chemical Shifts. A study of the temperature dependence of the chemical shifts was performed on all assigned ^1H and ^{13}C signals, working in the temperature range between 278 and 318 K. A fit of chemical shifts versus inverse temperature for each resonance to a linear equation provides a qualitative way to classify the trends as Curie, hyper-Curie, hypo-Curie, or *T*-independent, depending on the intercept and slope of the δ versus $1/T$ plot.[39] Almost none of the signals shows Curie behavior, and, as pointed out

previously,[27,30,31] this can be attributed to the presence of a low lying exicted state, which is populated at room temperature. The temperature dependence data were fitted to a two-state model using the program TDFw, by Shokhirev and Walker.[40] The energy gap between the ground and excited states is found to be 600 ± 200 cm^{-1}, with a variability of less than 10% when the calculation was performed by excluding any one of the resonances from the input data, supporting the robustness of the fit. We observe that, when only ^{1}H signals were used as input data, it was hard to achieve convergence, and the resulting parameters were highly variable.

Discussion

The analysis of NMR data arising from nuclei close to paramagnetic centers is of paramount importance as it yields valuable information about its electronic structure, complementing data available from EPR, ENDOR, and other spectroscopic techniques.[51,55] Usually, one main limitation to such studies is the excessive line broadening experienced by signals arising from nuclei that are too close to the paramagnetic center. Because broadening decreases with the square of the gyromagnetic ratio of the involved nucleus, the use of heteronuclei has been of great help for paramagnetic systems and large proteins.[51,56−62] Indeed, ^{13}C direct detection allowed us to observe all of the resonances of ^{13}C nuclei from the metal ligands in *Tt*Cu$_A$, even for those nuclei that are only two bonds away from the copper ions and contain a high degree of unpaired spin density, such as the Cys Cβs. No hyperfine-shifted ^{13}C resonances corresponding to the weak axial ligands Met160 and Gln151 were observed, in agreement with ^{1}H NMR data.[26−31,63]

We have shown that saturation transfer difference experiments on ^{13}C spectra are useful to obtain unambiguous assignments of the hyperfine shifted resonances, provided the assignments of the corresponding diamagnetic signals are available. We have also exploited the assignment of paramagnetic ^{13}C resonances to unambiguously assess the identity of paramagnetic ^{1}H signals through ^{1}H,^{13}C-HMQC and ^{13}C-edited ^{1}H spectra. By using this approach, we achieved a full assignment of the paramagnetic ^{1}H and ^{13}C spectra of *Tt*Cu$_A$. This includes the sequence-specific assignment of the Cys resonances, despite their extremely broad line widths.

The chemical shifts of resonances assigned to ligand nuclei in the paramagnetic species contain information about the degree of unpaired spin density delocalized onto the observed nuclei.[55,64] Table 2 reports the observed chemical shifts and the calculated apparent hyperfine coupling constant $(A/h)_{app}$ for each nucleus (see Materials and Methods). These data further confirm the high degree of delocalization of the electron spin density on the Cys ligands of the *Tt*Cu$_A$ site. Analysis of the ^{13}C resonances shows sign alternation in the $(A/h)_{app}$ value for the three carbon nuclei in both Cys ligands, revealing the existence of spin polarization. This phenomenon was also observed for the Cys ligands in Fe(II) rubredoxin by Markley and co-workers.[56] The ^{1}H and ^{13}C line widths show a good correlation with $(A/h)_{app}^2$, while the correlation with r^{-6} is poor. This confirms that relaxation is mostly governed by a contact mechanism, as also reported for Cu(II) blue copper proteins.[65]

The availability of the $(A/h)_{app}$ for all ^{13}C and ^{1}H nuclei from the Cys ligands allows us to estimate the spin density on each residue. Despite that spin polarization effects preclude obtaining a precise figure,[64] it is evident that Cys153 bears a larger electron spin density as compared to Cys149 (Table 2). The available high-resolution structures of Cu$_A$ sites reveal some variability in the Cu−S distances (2.25−2.47 Å) within each protein,[7,66,67] in agreement with the unusually large Debye−Waller terms from EXAFS data.[21] However, none of these techniques is able to provide evidence for a stronger interaction with one particular Cys ligand, as we show here. The finding of net electron spin density on the NH from Gly115 (displaying an $(A/h)_{app}$ of −0.53 MHz), arising from a hydrogen bond between this moiety and

Table 2. Analysis of ^{1}H and ^{13}C NMR Chemical Shifts[a]

resonance	signal	δ_{obs} (ppm)	$\delta_{diamagnetic}$[b] (ppm)	$\delta_{pseudocontact}$[c] (ppm)	$\delta_{contact}$[c] (ppm)	$(A/h)_{app}$[c] (MHz)
			Cys149			
Cβ	Y	−379.4	32.3	−3.99	−407.7	−3.67
Cα	F	294.6	59.9	−1.38	236.1	2.12
Hβ	b	262	3.05	−2.58	261.5	9.37
Hβ	c	237	3.32	−2.58	236.3	8.48
Hα	y	−2.9	4.41	−1.10	−6.2	−0.22
CO	I	151.7	176.3	−1.21	−23.4	−0.21
			Cys153			
Cβ	Z	−475.3	34.5	−3.4	−506.4	−4.56
Cα	A	880.5	56.5	−1.36	825.4	7.43
Hβ	a	283	2.89	−3.26	283.4	10.15
Hβ	d	117	3.08	−3.26	117.2	4.21
Hα	g	27.55	4.54	−2.6	25.6	0.92
CO	J	142.0	174.4	−0.80	−31.6	−0.28
			His114			
Cε1	M	33.9	137.9	−2.06	−101.9	−0.92
Cδ2	C	353.6	120.2	−0.74	234.1	2.11
Cγ	E	312.2	135.5	−1.51	178.2	1.60
Hδ2	e	31.6	6.66	−0.4	25.3	0.91
Hε2	h	24.2	11.78	−0.56	13.0	0.46
Hε1	j	20.7	6.97	−2.19	15.9	0.57
			Gly115			
HN	z	−5.2	10.1	−0.57	−14.7	−0.53
			His157			
Cε1	L	98.4	140.6	−2.23	−40	−0.36
Cδ2	B	386.2	119.0	−0.86	268.1	2.41
Cγ	D	331.2	136.5	−1.75	196.4	1.77
Hδ2	f	27.46	7.31	−0.49	20.6	0.74
Hε2	i	23.2	10.0	−0.61	13.8	0.49
Hε1	k	15.5	7.38	−2.28	10.4	0.37

[a] Data reported and calculated at 298 K. [b] Taken from the assignment reported for reduced *Tt*CuA in BMRB ID 5819.[54] [c] Calculated as indicated in Materials and Methods.

(55) Bertini, I.; Turano, P.; Vila, A. J. *Chem. Rev.* **1993**, *93*, 2833–2932.
(56) Machonkin, T. E.; Westler, W. M.; Markley, J. L. *Inorg. Chem.* **2005**, *44*, 779–797.
(57) Kostic, M.; Pochapsky, S. S.; Pochapsky, T. C. *J. Am. Chem. Soc.* **2002**, *124*, 9054–9055.
(58) Xia, B.; Westler, W. M.; Cheng, H.; Meyer, J.; Moulis, J.-M.; Markley, J. L. *J. Am. Chem. Soc.* **1995**, *117*, 5347–5350.
(59) Bermel, W.; Bertini, I.; Felli, I. C.; Kummerle, R.; Pierattelli, R. *J. Am. Chem. Soc.* **2003**, *125*, 16423–16429.
(60) Bertini, I.; Felli, I. C.; Luchinat, C.; Parigi, G.; Pierattelli, R. *ChemBioChem* **2007**, *8*, 1422–1429.
(61) Bermel, W.; Bertini, I.; Felli, I. C.; Matzapetakis, M.; Pierattelli, R.; Theil, E. C.; Turano, P. *J. Magn. Reson.* **2007**, *188*, 301–310.
(62) Bermel, W.; Bertini, I.; Felli, I.; Piccioli, M.; Pierattelli, R. *Prog. Nucl. Magn. Reson. Spectrosc.* **2006**, *48*, 25–45.
(63) Dennison, C.; Berg, A.; De Vries, S.; Canters, G. W. *FEBS Lett.* **1996**, *394*, 340–344.
(64) Bertini, I.; Luchinat, C. *NMR of Paramagnetic Molecules in Biological Systems*; Benjamin/Cummings: Menlo Park, CA, 1986.
(65) Bertini, I.; Ciurli, S.; Dikiy, A.; Gasanov, R.; Luchinat, C.; Martini, G.; Safarov, N. *J. Am. Chem. Soc.* **1999**, *121*, 2037–2046.
(66) Robinson, H.; Ang, M. C.; Gao, Y. G.; Hay, M. T.; Lu, Y.; Wang, A. H. *Biochemistry* **1999**, *38*, 5677–5683.
(67) Brown, K.; Djinovic-Carugo, K.; Haltia, T.; Cabrito, I.; Saraste, M.; Moura, J. J.; Moura, I.; Tegoni, M.; Cambillau, C. *J. Biol. Chem.* **2000**, *275*, 41133–41136.

the S atom of Cys149, may account for this difference, because the S atom of Cys153 is not involved in any hydrogen bond. Inspection of the reported X-ray structures[7,68−70] reveals that this hydrogen bond (between Cys149 and the residue adjacent to the N-terminal His ligand) is conserved in all structurally characterized native Cu_A centers, including C*c*Os and N_2O reductases, thus implying it is an essential structural feature. This situation resembles the H-bond between a highly conserved Asn residue and the Cys ligand in blue copper proteins. For blue copper proteins, the *A*/*h* value for this NH ranges between −0.8 and −1.3 MHz, which has been shown to reflect the electron spin density on the sulfur atom of the Cys residue, on its turn modulated by the interaction with the axial ligand and/or the geometry of the metal center.[31,65,71−73] The herein reported value of −0.53 MHz is in agreement with the observation that both Cys ligands in Cu_A sites bear an electron spin density half of that observed for Cu(II)-bound Cys ligands in type I centers.

This conserved hydrogen bond is formed with a peptide NH group; thus it is not possible to remove it by site-directed mutagenesis. However, inspection of the structural data of engineered Cu_A sites aids in assessing its role. Loop-directed mutagenesis has been employed to engineer a Cu_A center into azurin[74] and into subunit II of *E. coli* quinol oxidase (CyoA).[75] Cu_A-azurin, which displays the typical spectral features of delocalized mixed-valence Cu_A centers, preserves this H-bond,[66] while the CyoA center shows some degree of valence localization[34] and lacks this H-bond.[75] This H-bond is not located in any of the possible electron transfer pathways in which the Cu_A center is involved, allowing us to discard a possible role of this moiety in the donor−acceptor coupling. Therefore, we propose that this H-bond is important to maintain the electronic structure (and the mixed-valence nature) of the center, possibly by tuning the redox potential of the metal site, as observed in blue copper and iron−sulfur centers.[76−78]

Previous NMR studies have indicated the nonequivalence of the two His ligands in Cu_A sites.[26−31,63] Analysis of different high-resolution crystal structures of native and engineered Cu_A centers led Lu and co-workers to propose that the copper−axial ligand distances determine the orientation of the His imidazole rings and therefore the His nonequivalence.[66] Now we provide evidence that the Cys ligands are also nonequivalent. This piece of evidence cannot be derived from other spectroscopies, which cannot distinguish each Cys−Cu bond.

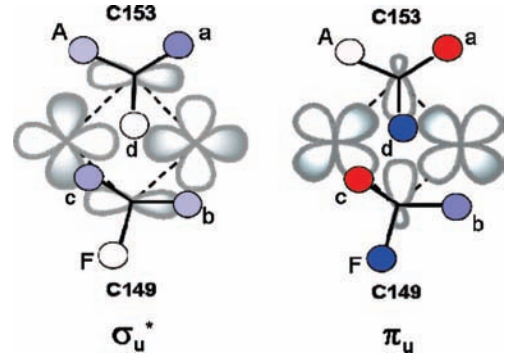

Figure 5. Schematic representation of the AO involved in the σ^*_u and π_u states. The d orbitals from the copper ions and the p orbitals from the S atoms are shown. Labels correspond to NMR resonances, as detailed in Table 1.

The sequence-specific assignment of all Cys resonances allows us to analyze the angular dependence of their chemical shifts, which are expected to reflect the electron spin density on the sulfur atoms.[79,80] The $(A/h)_{app}$ values observed for the four Cys Hβs should follow a sine-squared or cosine-squared relationship with the S−S−Cβ−Hβ dihedral angles, which is not the case here. As was already discussed by Salgado, Canters, and co-workers, this apparent disagreement can be explained by assuming that NMR is monitoring a temperature-averaged population of two states.[27] Here, we have resorted to the temperature dependence of the chemical shifts to retrieve information on the excited state,[40] based on the complete and unambiguous assignment of the ^{1}H and ^{13}C resonances. In particular, inclusion of the sharper ^{13}C signals in the fit allows a robust data analysis. This resulted in an energy gap of 600 ± 200 cm^{-1} between the ground state and a temperature-accessible excited state, in agreement with previous estimates.[27] From this value, a population of 2 −12.5% is expected for the excited state at room temperature, and 3.2−15.5% at the growth temperature of *Thermus thermophilus* (341 K).

The σ^*_u and π_u states differ by the involvement of d_{x2-y2} and d_{xy} orbitals from the copper ions, respectively (Figure 5).[27] Thus, the angular dependence of the *A*/*h* values with the S−S−Cβ−Hβ dihedral angles should follow a sine-squared dependence for the σ^*_u state, and a cosine-squared dependence for the π_u level. Analysis of the *A*/*h* values estimated for the ground state and the excited state for the different ^{1}H and ^{13}C resonances (Supporting Information, Table S1) confirms that the room-temperature electronic structure of the Cu_A center is a thermal average of a σ^*_u ground state and a π_u excited state, and accounts for the anomalous temperature dependence of the hyperfine shifts. For instance, in Cys149, the sulfur p_x orbital in the ground state lays almost perpendicular to the Cβ−Cα bond, while in the excited state this bond and the contributing sulfur p_y orbital are almost collinear. Therefore, the ^{13}C nucleus (signal F) in the π_u level is expected to experience a much larger electron spin density than in the σ^*_u state, and thus higher temperatures lead to higher δ_{con} shifts, inducing a markedly anti-Curie behavior. For the Cα of Cys153 (signal A), the reversal

(68) Iwata, S.; Ostermeier, C.; Ludwig, B.; Michel, H. *Nature* **1995**, *376*, 660–667.
(69) Qin, L.; Hiser, C.; Mulichak, A.; Garavito, R. M.; Ferguson-Miller, S. *Proc. Natl. Acad. Sci. U.S.A.* **2006**, *103*, 16117–16122.
(70) Brown, K.; Tegoni, M.; Prudencio, M.; Pereira, A. S.; Besson, S.; Moura, J. J.; Moura, I.; Cambillau, C. *Nat. Struct. Biol.* **2000**, *7*, 191–195.
(71) Donaire, A.; Jimenez, B.; Fernandez, C. O.; Pierattelli, R.; Kohzuma, T.; Moratal, J. M.; Hall, J. F.; Kohzuma, T.; Hasnain, S. S.; Vila, A. J. *J. Am. Chem. Soc.* **2002**, *124*, 13698–13708.
(72) Bertini, I.; Ciurli, S.; Dikiy, A.; Fernandez, C. O.; Luchinat, C.; Safarov, N.; Shumilin, S.; Vila, A. J. *J. Am. Chem. Soc.* **2001**, *123*, 2405–2413.
(73) Bertini, I.; Fernandez, C. O.; Karlsson, B. G.; Leckner, J.; Luchinat, C.; Malmström, B. G.; Nersissian, A. M.; Pierattelli, R.; Shipp, E.; Valentine, J. S.; Vila, A. J. *J. Am. Chem. Soc.* **2000**, *122*, 3701–3707.
(74) Hay, M.; Richards, J. H.; Lu, Y. *Proc. Natl. Acad. Sci. U.S.A.* **1996**, *93*, 461–464.
(75) Wilmanns, M.; Lappalainen, P.; Kelly, M.; Sauer-Eriksson, E.; Saraste, M. *Proc. Natl. Acad. Sci. U.S.A.* **1995**, *92*, 11955–11959.
(76) Hoitink, C. W.; Canters, G. W. *J. Biol. Chem.* **1992**, *267*, 13836–13842.
(77) Dong, S.; Ybe, J. A.; Hecht, M. H.; Spiro, T. G. *Biochemistry* **1999**, *38*, 3379–3385.
(78) Dey, A.; Jenney, F. E., Jr.; Adams, M. W.; Babini, E.; Takahashi, Y.; Fukuyama, K.; Hodgson, K. O.; Hedman, B.; Solomon, E. I. *Science* **2007**, *318*, 1464–1468.
(79) Bertini, I.; Capozzi, F.; Luchinat, C.; Piccioli, M.; Vila, A. J. *J. Am. Chem. Soc.* **1994**, *116*, 651–660.
(80) Bertini, I.; Donaire, A.; Feinberg, B. A.; Luchinat, C.; Piccioli, M.; Yuan, H. *Eur. J. Biochem.* **1995**, *232*, 192–205.

situation is met, resulting in a hyper-Curie behavior. The same reasoning applies to the ^{1}H resonances if we consider the sequence-specific assignment here reported. The chemical shifts of the β ^{13}C resonances should not be affected by this angular component, in agreement with the similar *A*/*h* values estimated for the ground and excited states. Overall, these data unequivocally confirm that the excited state populated at room temperature is a π_u.

Neese and co-workers provided the first experimental evidence of a σ^*_u ground state for Cu_A sites,[34,35] later supported by further spectroscopic data and theoretical calculations.[17,19,33] Solomon and co-workers have proposed that this state is stabilized by the protein environment, resulting in a short Cu−Cu distance (2.4−2.6 Å).[33] Instead, the mixed valence compound synthesized by the Tolman group displays a π_u ground state, dictated by its longer Cu−Cu distance (3.0 Å).[19] Solomon has recently proposed that the thermal equilibrium between the σ^*_u and π_u levels that accounts for the NMR data takes place along an almost flat energy surface, where the Cu−Cu distance is expected to undergo a variation of 0.5 Å.[33] The observation of a single NMR line for all ^{1}H and ^{13}C resonances in all Cu_A sites at different magnetic fields suggests that the equilibrium between these two states is fast on the NMR time scale. The chemical shift differences estimated for ^{1}H nuclei in both states are as high as 2000 ppm (Supporting Information, Table S1), which suggests a lower limit of 1.2×10^6 s^{-1} for the exchange rate. These rates (despite small for vibrational frequencies) seem unlikely for a change in the Cu−Cu distance of 0.5 Å. We therefore favor an alternative interpretation: different theoretical calculations have revealed that small changes in the Cu−Cu distance in Cu_A sites strongly affect the energy gap between these two levels.[19,36,81] A slightly longer Cu−Cu distance (2.6−2.7 Å), which may be achieved at room temperature, is consistent with a σ^*_u/π_u energy gap close to the value here determined. EXAFS data have revealed a significant increase in the Cu−Cu Debye−Waller terms in spectra recorded at higher temperatures,[21] in agreement with this proposal. Therefore, EPR and NMR data can be reconciled by assuming a decrease in this energy difference from 3500−5000 cm^{-1} at cryogenic temperatures to a value of 600 cm^{-1} at room temperature, induced by a minor geometric change in the Cu_2S_2 core.

Recent NMR studies[37,38] have highlighted the role of thermally populated (from 0.5 to 10%), "invisible" excited states of proteins at room temperature, which may play a role in enzyme catalysis, ligand binding, and protein folding. The precise characterization of a low-lying excited state that contributes to the electronic structure of the Cu_A site suggests that this state may also play a role in electron transfer.

Acknowledgment. L.A.A. and G.N.L. thank CONICET for doctoral and postdoctoral fellowships, respectively. A.J.V. is a staff member from CONICET and an HHMI International Research Scholar. This work was supported by the U.S. National Institutes of Health (R01-GM068682) and Agencia Nacional de Promoción Científica y Tecnológica (PICT2002-01-11625) grants to A.J.V. This work has been supported in part by the EC contracts EU-NMR (no. 026145) and SPINE II (no. 031220) and by Ente Cassa di Risparmio di Firenze. The Bruker Avance II 600 MHz NMR spectrometer at Rosario was purchased with funds from ANPCyT (PME2003-0026) and CONICET. We thank Prof. John Markley for kindly providing us with the *E. coli* JM15 (DE3) pLysS cells and Prof. Ivano Bertini for stimulating discussions.

Supporting Information Available: Table S1, *A*/*h* values calculated at 298 K for the ground and excited states using the output from the fits performed with the program TDF;[40] Figure S1, zoom on the f, g, and y signals of the ^{1}H NMR spectra of unlabeled and selectively ^{13}C,^{15}N labeled Cys *Tt*Cu_A samples registered at 288 K; Figure S2, ^{1}H,^{13}C HMQC spectrum of uniformly labeled *Tt*Cu_A; Figure S3, ^{1}H NMR spectra acquired with selective irradiation of ^{13}C resonances B and C fit; Figure S4, ^{13}C-filtered ^{1}H spectra registered on a sample of *Tt*Cu_A labeled at Cys with the offset at 300 and 800 ppm; Figure S5, ^{1}H NOE experiments on resonances a−d; Figure S6, ^{1}H saturation transfer difference experiments on resonances a−d; Figure S7, ^{1}H saturation transfer difference experiment on resonance z; Figure S8, plot showing experimental data of chemical shift versus temperature dependence together with the fits perfomed with the program TDF. This material is available free of charge via the Internet at http://pubs.acs.org.

JA8079669

(81) Neese, F. Electronic Structure and Spectroscopy of Novel Copper Chromophores in Biology. Ph.D. Dissertation, University of Konstanz, 1996.